

$K^+$  p Elastic Scattering at 3.5 and 5.0 GeV/c

W. De Baere, J. Debaisieux, P. Dufour, F. Grard, J. Heughebaert, L. Pape,  
P. Peeters, F. Verbeure, and R. Windmolders.

Laboratoire des Hautes Energies, Bruxelles.

R. George<sup>+</sup>, Y. Goldschmidt-Clermont, V.P. Henri, B. Jongejans, D.W.G. Leith<sup>++</sup>,  
A. Moisseev<sup>+++</sup>, F. Muller<sup>++++</sup>, J.M. Perreau and V. Yarba<sup>+++</sup>.

CERN, Geneva.

---

Abstract

The elastic scattering of  $K^+$  mesons on protons is studied at 3.5 and 5 GeV/c. The total elastic cross sections are found to be  $(4.36 \pm 0.36)$ mb and  $(3.82 \pm 0.41)$ mb respectively. The differential elastic cross section, which exhibit characteristic diffraction peaks, are fitted by:

$$\frac{d\sigma}{dt} = \left( \frac{d\sigma}{dt} \right)_0 e^{\alpha t}$$

giving  $\alpha = 3.85 \pm 0.12$  and  $4.70 \pm 0.21$  (GeV/c)<sup>-2</sup> for the two momenta respectively, with  $|t| \approx 0.65$  (GeV/c)<sup>2</sup>. The results are compared to those at neighbouring energies, giving some support to the presence of a real part of the forward scattering amplitude. The diffraction peak shows definite shrinking with increasing momenta. The data are examined in the light of models for high energy scattering.

---

+ Now at Institut du Radium, Paris.

++ Now at Stanford Linear Accelerator Centre, Stanford, California.

+++ On leave of absence from Joint Institute for Nuclear Research, Dubna.

++++ On leave of absence at Ecole Polytechnique, Paris.

The  $K^+p$  elastic scattering reaction was studied at 3.0, 3.5 and 5.0 GeV/c as part of a systematic bubble chamber investigation of  $K^+p$  interactions. The film was obtained in exposures of the 81 cm Saclay hydrogen bubble chamber in a separated  $K^+$  beam from the CERN proton-synchrotron. The details of the exposure and analysis of elastic scattering at 3.0 GeV/c have been published<sup>(1)</sup>, and preliminary results at all three momenta were given at Dubna, 1964<sup>(2)</sup>. Here, the results at 3.5 and 5.0 GeV/c are presented and a comparison is made with the other available  $K^+p$  scattering data, and theoretical models.

The beam momenta were precisely determined for each experiment by measuring and fitting three-prong events to the  $\tau$ -decay hypothesis ( $K^+ \rightarrow \pi^+ \pi^- \pi^+$ ). The best values for the momenta at the centre of the chamber were found to be 3.46 and 4.97 GeV/c, respectively, with a spread of  $\pm 1/2$  %. The beam contamination by pions was less than 5 % at 3.5 GeV/c and 5.0 GeV/c.

About 80,000 pictures at 3.5 GeV/c and 40,000 pictures at 5.0 GeV/c were scanned for events of the two-prong topology. The events in a fiducial volume were measured and passed through the standard CERN computer programs; they finally yielded a sample of 2949 identified elastic events at 3.5 GeV/c and 1436 events at 5.0 GeV/c. The experimental biases were investigated and appropriate corrections were made as in the 3 GeV/c experiment<sup>(1)</sup>: only events with the cosine of the scattering angle less than 0.99, (corresponding to a proton range of  $\sim 1.5$  cm at 3.5 GeV/c and  $\sim 3.5$  cm at 5.0 GeV/c) and with a dip angle less than  $80^\circ$ , were accepted for the analysis. (The dip angle is defined as the angle between the scattering plane and the chamber window). Additional cuts in the dip angle, were imposed on those events with the cosine of the scattering angle smaller than 0.98 (see Table I)

The angular distributions for  $K^+p$  elastic scattering at 3.5 and 5.0 GeV/c (after correction for the cuts mentioned, on the basis of the expected isotropic azimuthal distribution) are given in Table I and are shown in Fig. 1 for small angles. The experimental distributions show

a characteristic forward diffraction peak of approximately exponential shape. They were fitted by the following functions, using the maximum-likelihood program MALIK<sup>(3)</sup>:

$$\frac{d\sigma}{dt} = \left(\frac{d\sigma}{dt}\right)_0 e^{\alpha t} \quad (1)$$

$$\frac{d\sigma}{dt} = \left(\frac{d\sigma}{dt}\right)_0 e^{\alpha t + \beta t^2} \quad (2)$$

and the values of  $\left(\frac{d\sigma}{dt}\right)_0$  and of the parameters  $\alpha$  and  $\beta$  are given in Table II for two different ranges of the square of the momentum transfer  $t$ . As the table shows, there is a small indication of backward scattering.

The elastic scattering cross sections were determined from the corrected number of events, using the extrapolation to zero angle by the above fits and allowing for the scanning efficiency determined by repeated scanning. The total  $K^+$  path length scanned was determined from the number of  $\tau$ -decays ( $K^+ \rightarrow \pi^+ \pi^- \pi^+$ ), observed within the same fiducial volume as the two-prong events, and using the branching fraction of 0.055 and the  $K^+$  lifetime  $(1.229 \pm 0.008) \times 10^{-8}$  sec.<sup>(4)</sup> The effect of the beam contamination could be neglected, as discussed previously<sup>(1)</sup>. The elastic cross sections were found to be  $(4.36 \pm 0.36)$ mb, and  $(3.82 \pm 0.41)$ mb at 3.5 GeV/c and 5.0 GeV/c, respectively. They are shown together with data from other experiments<sup>(5)-(13)</sup> in Fig. 2. The total cross section is also displayed.

The forward scattering cross-section was calculated by extrapolation to  $0^\circ$  of the angular distribution data. The one-parameter fit, when used for  $|t| \gtrsim 0.65$ , gives  $\left(\frac{d\sigma}{dt}\right)_0 = (16.6 \pm 1.5)$  and  $(17.9 \pm 1.9)$ mb/(GeV/c)<sup>2</sup> at 3.5 and 5.0 GeV/c respectively, the two-parameter fit over a wider range of  $t$  gives  $(16.4 \pm 1.6)$  and  $(18.4 \pm 2.3)$ mb/(GeV/c)<sup>2</sup>. These values lie somewhat above the "optical point", and although the errors are large, they confirm the result from the 3.0 GeV/c data<sup>(1)</sup>. The "optical point" as derived from the optical theorem, in the limiting case of purely

imaginary forward scattering amplitude

$$\left(\frac{d\sigma}{dt}\right)_{\text{opt}} = \frac{1}{16\pi h^2 c^2} \sigma_{\text{T}}^2$$

is computed for all values of the total cross section  $\sigma_{\text{T}}$  shown on Fig. 2, and plotted on Fig. 3 together with the values of the extrapolated forward experimental cross section obtained in the present and other neighbouring experiments (1)(7)(12)(13). It is seen that, although each individual determination is subject to appreciable experimental errors, the experimental points all lie above the optical points, indicating the presence of a real component of the forward scattering amplitude. In particular, if the interpolated value of  $\sigma_{\text{T}} = 17.2 \pm 0.3$  mb (see Fig. 2) is adopted for the total cross section at 3.5 GeV/c and 5.0 GeV/c, the values  $|\text{Rea}/\text{Ima}| = 0.31 \pm 0.21$  at 3.5 GeV/c and  $0.45 \pm 0.14$  at 5.0 GeV/c are found, using the one-parameter fit.

The momentum dependence of the slope of the diffraction peak is summarized in Fig. 4, where the parameters  $\alpha$  and  $\beta$  are plotted separately. The figure shows an initial shrinking of the diffraction peak in the region of 2 to 5 GeV/c, which is probably correlated with the fact that the inelastic cross section changes rapidly in this region while the total cross section remains constant. The region above 5 GeV/c is characterised by a slow shrinking, almost linear with the incident  $K^+$  momentum.

The model of van Hove<sup>(14)</sup>, in its simplest form, assumes a purely imaginary elastic scattering amplitude, and an overlap function of the form  $\exp(-At)$ . In this case, the quantities  $\sigma_{\text{T}}$ ,  $\sigma_{\text{E}}$ ,  $\alpha$  and  $\beta$  are determined by given functions of  $A$  and of a parameter  $f_0$ , with range  $0 \leq f_0 \leq 1/2$ . In particular, the ratio  $\sigma_{\text{E}}/\sigma_{\text{T}}$  is an increasing function of  $f_0$  and reaches the value 0.185 for the upper limit. The experimental values of the ratio are displayed on Fig. 5, and its upper bound predicted by the model is shown as a dotted line. On Fig. 4, the dotted lines represent the corresponding values of  $\alpha$  and  $\beta$ . At the incident momenta of the present experiment, the ratio  $\sigma_{\text{E}}/\sigma_{\text{T}}$  and the parameter  $\alpha$  have not yet reached their high energy limits. However, it can be seen that the

experimental values are already rapidly approaching the limits at the relatively low momentum of 5 GeV/c, and then remain constant. Thus it may be concluded that the  $K^+p$  elastic scattering approaches an asymptotic behaviour at rather lower energies than, for instance,  $\bar{p}p$  or  $\pi p$  elastic scattering.

This nearly asymptotic behaviour justifies an attempt to compare the experimental data with models developed for the interpretation of high energy scattering. For instance, Phillips and Rarita<sup>(15)</sup> fitted all previously available high energy data on scattering and charge exchange for  $\pi^\pm N$  and  $K^\pm N$  using a Regge-pole model with 5 poles, with a semi-empirical parametrization of the trajectories and residue functions. Using the parameters given by these authors, the total and elastic cross sections, as well as the differential cross sections, were computed at the incident momenta of the present experiment. The agreement with the experimental data is remarkable, as shown by Fig. 6 for the cross sections and by Fig. 7 for the differential cross sections at 3, 3.5 and 5 GeV/c. The agreement is still acceptable, even at 2 GeV/c, with the data of Chinowsky et al.<sup>(12)</sup> (Fig. 7,d). These curves show that, although the dependence of the differential cross sections on  $|t|$  is appreciably different from the exponential forms (1) and (2), the agreement with experiment persists to the smallest measured values of  $|t|$ . It was checked that this also holds true for the measurements of Foley et al.<sup>(13)</sup> at higher incident momenta. It is interesting to note that the simultaneous agreement of the total cross sections, and of the differential elastic cross sections for small  $|t|$ , implies also an agreement with another feature of the Regge-pole model, the presence of a real part of the forward elastic scattering amplitude. It is not clear at this stage whether the successes of the model is partly fortuitous, as some high energy approximations used by the model may lose validity at such relatively low momenta as the one considered in this paper. None the less, if only as a parametrization of the experimental data, the fit of Phillips and Rarita is found to be accurate for  $K^+p$  over a large range of momenta\*.

---

\* Phillips and Rarita give several solutions for their fit, which all agree equally well with the present data.

Fruitful discussions with R. Armenteros, L. van Hove, J. Naisse and R.J.N. Phillips are gratefully acknowledged. The authors wish to thank the crews of the proton synchrotron, of the 81 cm bubble chamber, and of the computer for their continued help, as well as their scanning and measuring staff. They are grateful to C. Peyrou (CERN) and to L. Rosenfeld (Brussels) for their valuable interest and support.

References

- 1) J. Debaisieux, F. Grand, J. Heughebaert, L. Pape, R. Windmolders, R. George, Y. Goldschmidt-Clermont, V.P. Henri, D.W.G. Leith, G.R. Lynch, F. Muller, J.M. Perreau, G. Otter and P. Sällström. Nuovo Cimento, in the press.
- 2) J. Debaisieux, F. Grand, J. Heughebaert, L. Pape, R. Windmolders, R. George, Y. Goldschmidt-Clermont, V.P. Henri, D.W.G. Leith, G.R. Lynch, F. Muller, J.M. Perreau. Proceedings of the Dubna International Conference on High Energy Physics, 1964.
- 3) F. Grand. Nucl. Inst. Methods - 34, 242 (1965)
- 4) A.H. Rosenfeld, A. Barbaro-Galtieri, W.M. Barkas, P.L. Bastien, J. Kirz and M. Roos. Rev. Mod. Phys. 37, 633, 1964 and UCRL Report 8030 (Revised 1965).
- 5) T. Stubbs, M. Bradner, W. Chinowsky, G. Goldhaber, S. Goldhaber, W. Slater, D. Stork and M. Ticho. Phys. Rev. Letters 7, 188 (1961).
- 6) V. Cook, D. Keefe, L.T. Kerth, P.G. Murphy, W.A. Wenzel and T.F. Zipf. Phys. Rev. Letters 7, 182 (1961).
- 7) V. Cook, D. Keefe, L.T. Kerth, P.G. Murphy, W.A. Wenzel and T.F. Zipf. Phys. Rev. 129, 2743 (1963).
- 8) W.F. Baker, R.L. Cook, E.W. Jenkins, T.F. Kycia, R.H. Phillips and A.L. Read. Phys. Rev. 129, 2285 (1963).
- 9) W.F. Baker, E.W. Jenkins, T.F. Kycia, R.H. Phillips, A.L. Read, K.F. Riley and H. Rudermann. Proceedings of the Sienna Conference on High Energy Physics, 1963 p.634.
- 10) W. Galbraith, E.W. Jenkins, T.F. Kycia, B.A. Leontic, R.H. Phillips and A.L. Read. Phys. Rev. 130 B, 913 (1965).

/...

- 11) J.L. Brown, R.W. Bland, M.G. Bowler, G. Goldhaber, S. Goldhaber, A.H. Hirata, J.A. Kadyk, V.H. Seeger and G. Trilling,  
Report to the Dubna Conference on High Energy Physics, 1964 -  
See also UCRL 11,446.
- 12) W. Chinowsky, G. Goldhaber, S. Goldhaber, T.O'Halloran and B. Schwarzschild,  
Phys. Rev. 139 B, 1411 (1965).
- 13) K.J. Foley, S.J. Lindenbaum, W.L. Love, S. Ozaki, J.J. Russel and L.C.L. Yuan,  
Phys. Rev. Letters 11, 503 (1963).
- 14) L. van Hove,  
Theoretical Problems in Strong Interactions at High Energies -  
CERN Report 65-22. Also : Theory of Interactions of Elementary  
Particles in the GeV Region - Invited Talk at International Symposium  
on Electron and Photon Interactions at High Energies, Hamburg 1965.
- 15) R.J.W. Phillips and W. Rarita,  
Phys. Rev. 139 B, 1336 (1965).



Figure Captions

- Fig. 1. Differential cross-section for  $K^+p$  scattering at 3.5 and 5.0 GeV/c. The solid curve is a one-parameter fit for  $|t| < 0.65$ . The dotted curve is a two-parameter fit over a wider range of  $t$ . For  $|t| < 0.65$  the two curves overlap.
- Fig. 2. Total and elastic scattering cross-sections for  $K^+p$  as a function of incident momentum.
- Fig. 3. Forward differential cross-section computed from the optical theorem, and experimental values, as a function of incident momentum.
- Fig. 4. Momentum dependence of the parameters  $\alpha$  and  $\beta$  in a fit to the differential cross-section of the form  $e^{\alpha t + \beta t^2}$ . The dashed lines are the predictions of the van Hove model<sup>(14)</sup> for the maximum value of its parameter  $f_0$ .
- Fig. 5. Momentum dependence of the ratio  $\sigma_E/\sigma_T$  of elastic to total cross-section. The dotted line is the upper limit of this ratio in the van Hove model.<sup>(14)</sup>
- Fig. 6. The total and elastic scattering cross-sections are compared to the Regge-pole model of Phillips and Rarita<sup>(15)</sup>.
- Fig. 7. a, b, c) The experimental elastic scattering differential cross-sections at 3, 3.5 and 5.0 GeV/c compared to the predictions of Phillips and Rarita. The two curves correspond to their solutions 1 and 3.  
d) Same comparison at 2 GeV/c with the data of Chinowsky et al.<sup>(12)</sup>.

o                      o  
o

TABLE I

Observed numbers of events N, cut-off angles of dip  $\Delta_{\max}$  and differential cross-sections as a function of t.

cos $\theta$	3.5 GeV/c.				5.0 GeV/c.			
	-t	N	$\Delta_{\max}$	$\frac{d\sigma}{dt}$	-t	N	$\Delta_{\max}$	$\frac{d\sigma}{dt}$
	(GeV/c) <sup>2</sup>		°	mb(GeV/c) <sup>-2</sup>	(GeV/c) <sup>2</sup>		°	mb(GeV/c) <sup>-2</sup>
0.99 - 0.98	0.0407	220	60	15.75 $\pm$ 1.66	0.0622	204	70	14.23 $\pm$ 1.78
0.98 - 0.96	0.0815	464	80	12.50 $\pm$ 1.17	0.1247	313	80	9.64 $\pm$ 1.14
0.96 - 0.94	0.1358	356	80	9.59 $\pm$ 0.94	0.2076	224	80	6.84 $\pm$ 0.85
0.94 - 0.92	0.1901	283	80	7.62 $\pm$ 0.77	0.2906	145	80	4.42 $\pm$ 0.59
0.92 - 0.90	0.2444	205	80	5.52 $\pm$ 0.59	0.3735	89	80	2.72 $\pm$ 0.40
0.90 - 0.88	0.2988	200	80	5.38 $\pm$ 0.55	0.4564	77	80	2.35 $\pm$ 0.39
0.88 - 0.86	0.3531	158	80	4.25 $\pm$ 0.49	0.5393	41	80	1.25 $\pm$ 0.23
0.86 - 0.84	0.4074	111	80	2.99 $\pm$ 0.37	0.6222	29	80	0.88 $\pm$ 0.19
0.84 - 0.82	0.4617	125	80	3.37 $\pm$ 0.41	0.7052	17	80	0.52 $\pm$ 0.14
0.82 - 0.80	0.5160	94	80	2.53 $\pm$ 0.33	0.7881	20	80	0.61 $\pm$ 0.15
0.80 - 0.75	0.6111	147	80	1.58 $\pm$ 0.18	0.9329	22	80	0.268 $\pm$ 0.064
0.75 - 0.70	0.7469	104	80	1.12 $\pm$ 0.14	1.1402	7	80	
0.70 - 0.65	0.8827	43	80	0.46 $\pm$ 0.08	1.3475	3	80	
0.65 - 0.60	1.0184	33	80	0.35 $\pm$ 0.07	1.5548	1	80	
0.60 - 0.55	1.1542	14	80			-		
0.55 - 0.50	1.2900	9	80			-		
0.50 - 0.45	1.4258	3	80			-		
0.45 - 0.40	1.5616	3	80	0.056 $\pm$		-		
0.40 - 0.35	1.6974	2	80	0.010		-		
0.35 - 0.30	1.8332	3	80			-		0.049 $\pm$
0.30 - 0.25	1.9690	3	80			-		0.0014
0.25 - 0.20	2.1048	1	80			-		
0.20 - 0.15	2.2406	2	80			-		
0.15 - 0.10	2.3764	2	80			-		
0.10 - 0.05	2.5122	2	80			-		
0.05 - 0.00	2.6480	2	80			-		
-0.00 - -0.05	2.7838	2	80			-		
-0.05 - -0.10	2.9196	2	80			-		
-0.10 - -0.15	3.0554	2	80			-		
-0.15 - -0.20	3.1911	2	80			-		
-0.20 - -0.25	3.3269	1	80			-		
-0.25 - -0.30	3.4627	1	80			-		
-0.30 - -0.35	3.5985	1	80			-		
-0.35 - -0.40	3.7343	1	80			-		
-0.40 - -0.45	3.8701	1	80			-		
-0.45 - -0.50	4.0059	1	80			-		
-0.50 - -0.55	4.1417	1	80	0.0068 $\pm$		-		
-0.55 - -0.60	4.2775	1	80	0.0018		-		
-0.60 - -0.65	4.4133	1	80			-		
-0.65 - -0.70	4.5490	2	80			-		
-0.70 - -0.75	4.6848	2	80			-		
-0.75 - -0.80	4.8206	2	80			-		
-0.80 - -0.85	4.9564	2	80			-		
-0.85 - -0.90	5.0922	2	80		7.7738	1		
-0.90 - -0.95	5.2280	1	80					
-0.95 - -1.0	5.3638	4	80		8.1884	2		

TABLE II

Fits to the differential cross-section

		3.46 GeV/c.		4.97 GeV/c.	
$\frac{d\sigma}{dt} = \left(\frac{d\sigma}{dt}\right)_0 \exp(\alpha t)$					
t	(GeV/c) <sup>2</sup>	0.027 <  t  < 0.679	0.027 <  t  < 1.847	0.041 <  t  < 0.622	0.041 <  t  < 1.658
$\left(\frac{d\sigma}{dt}\right)_0$	mb(GeV/c) <sup>-2</sup>	16.6 $\pm$ 1.5	16.8 $\pm$ 1.5	17.9 $\pm$ 1.9	17.8 $\pm$ 1.8
$\alpha$	(GeV/c) <sup>-2</sup>	3.85 $\pm$ 0.12	3.91 $\pm$ 0.08	4.70 $\pm$ 0.21	4.68 $\pm$ 0.14
$\frac{d\sigma}{dt} = \left(\frac{d\sigma}{dt}\right)_0 \exp(\alpha t + \beta t^2)$					
t	(GeV/c) <sup>2</sup>	0.027 <  t  < 1.086	0.027 <  t  < 1.847	0.041 <  t  < 1.036	0.041 <  t  < 1.658
$\left(\frac{d\sigma}{dt}\right)_0$	mb(GeV/c) <sup>-2</sup>	17.0 $\pm$ 1.8	16.4 $\pm$ 1.6	18.9 $\pm$ 2.7	18.4 $\pm$ 2.3
$\alpha$	(GeV/c) <sup>-2</sup>	4.10 $\pm$ 0.29	3.73 $\pm$ 0.21	5.24 $\pm$ 0.45	4.94 $\pm$ 0.36
$\beta$	(GeV/c) <sup>-4</sup>	0.33 $\pm$ 0.33	-0.17 $\pm$ 0.19	0.72 $\pm$ 0.55	0.29 $\pm$ 0.36

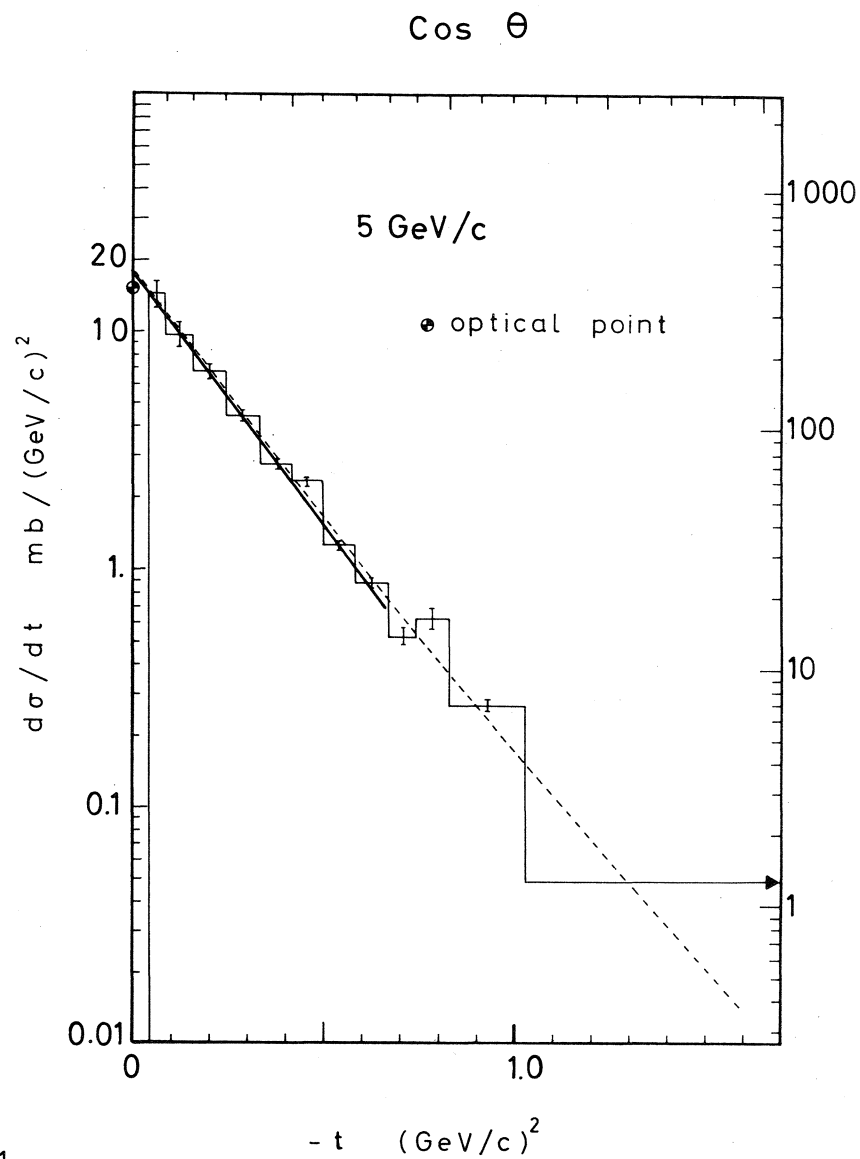
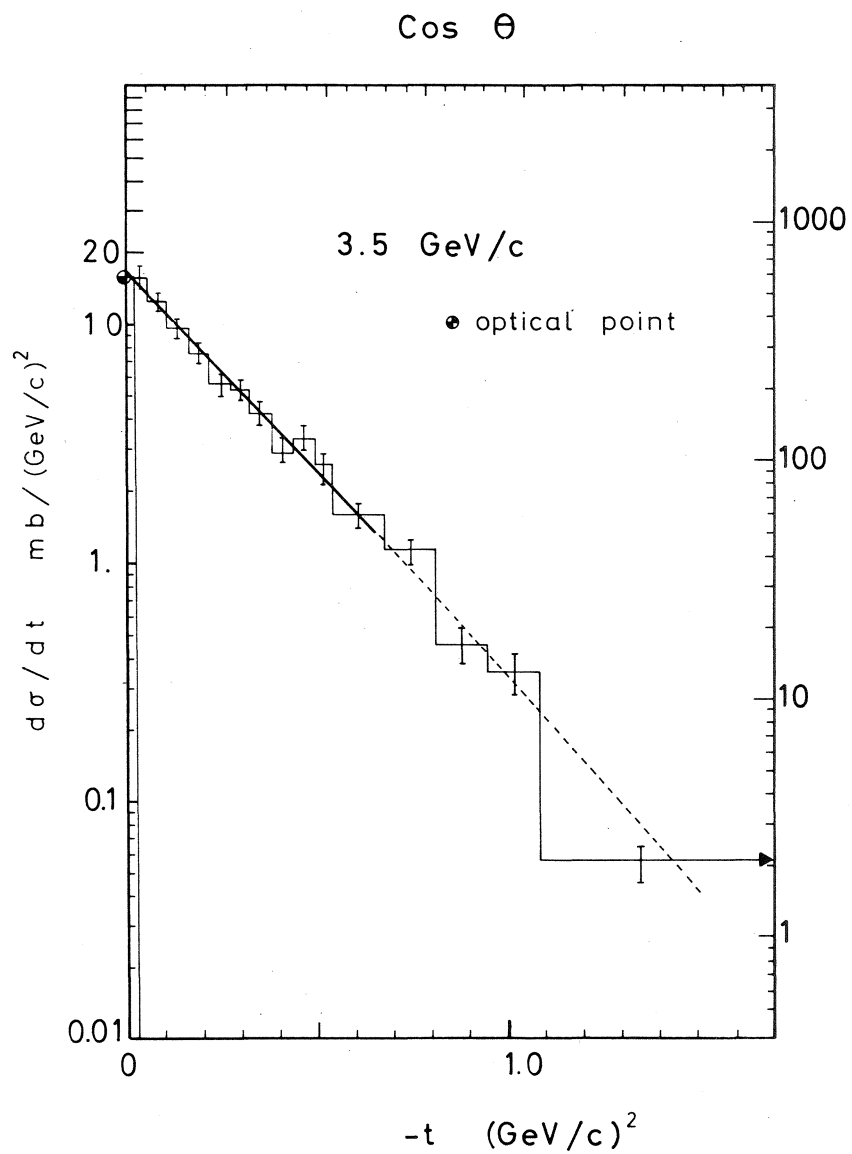


fig. 1

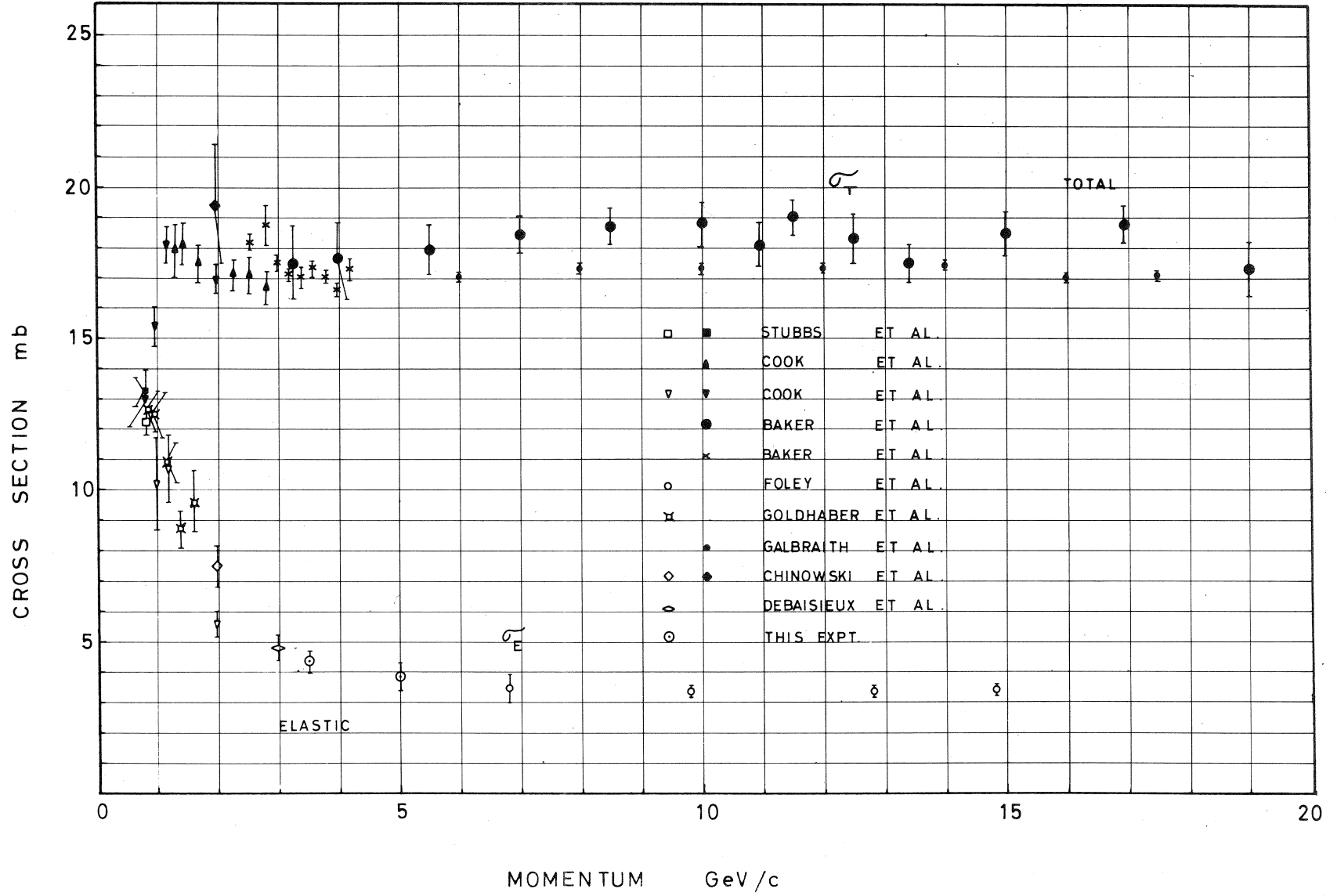


fig. 2

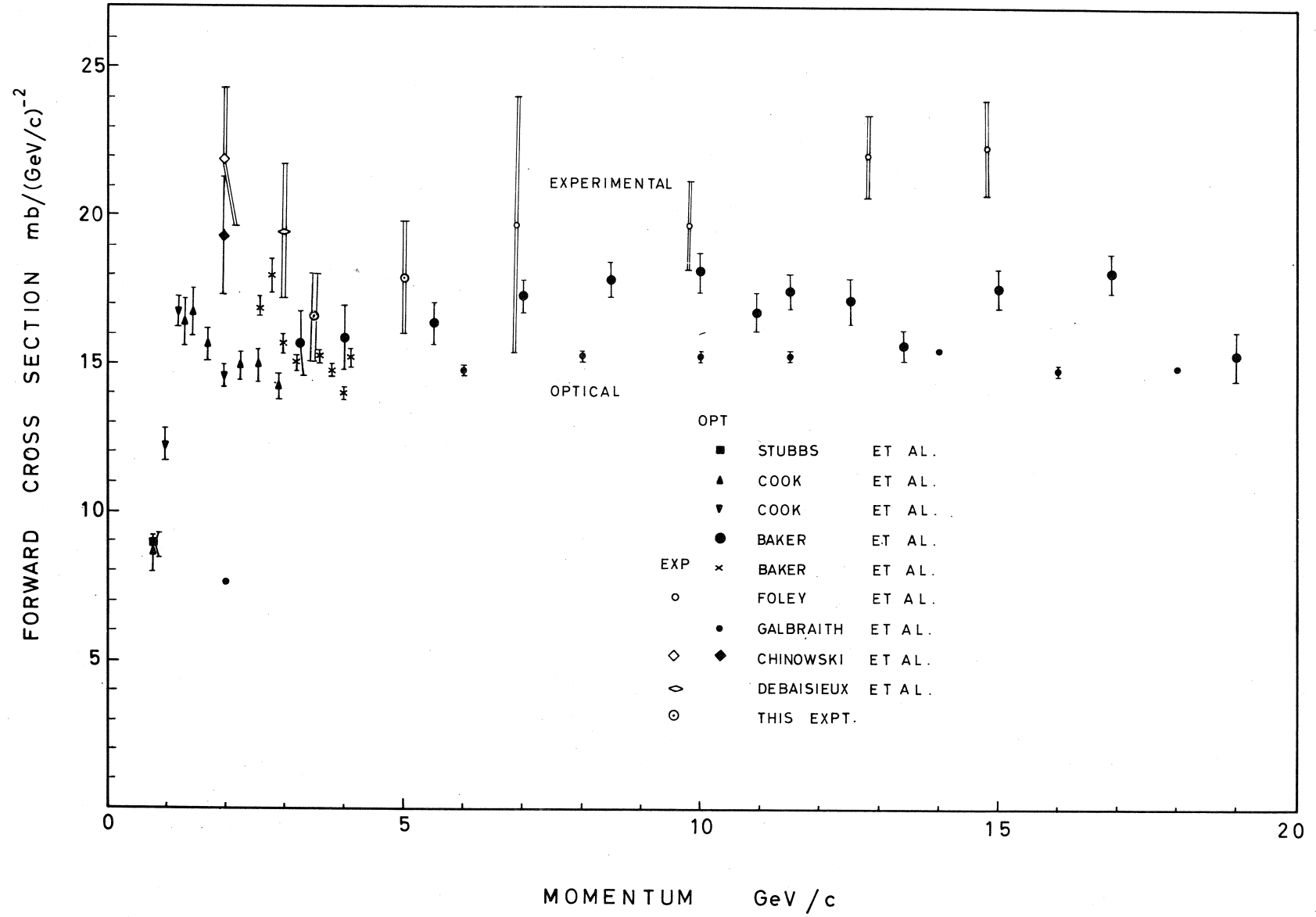


fig. 3

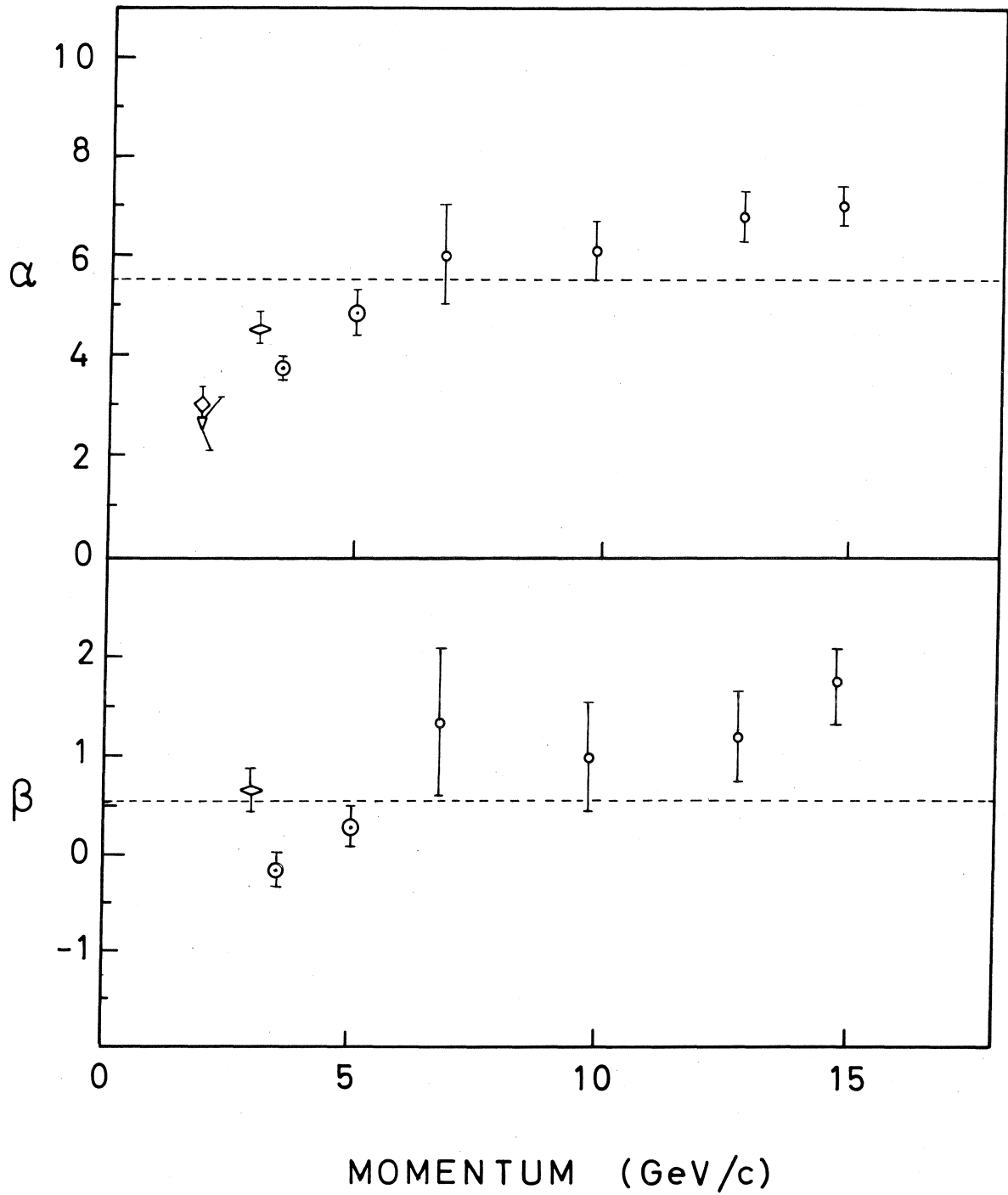


fig. 4

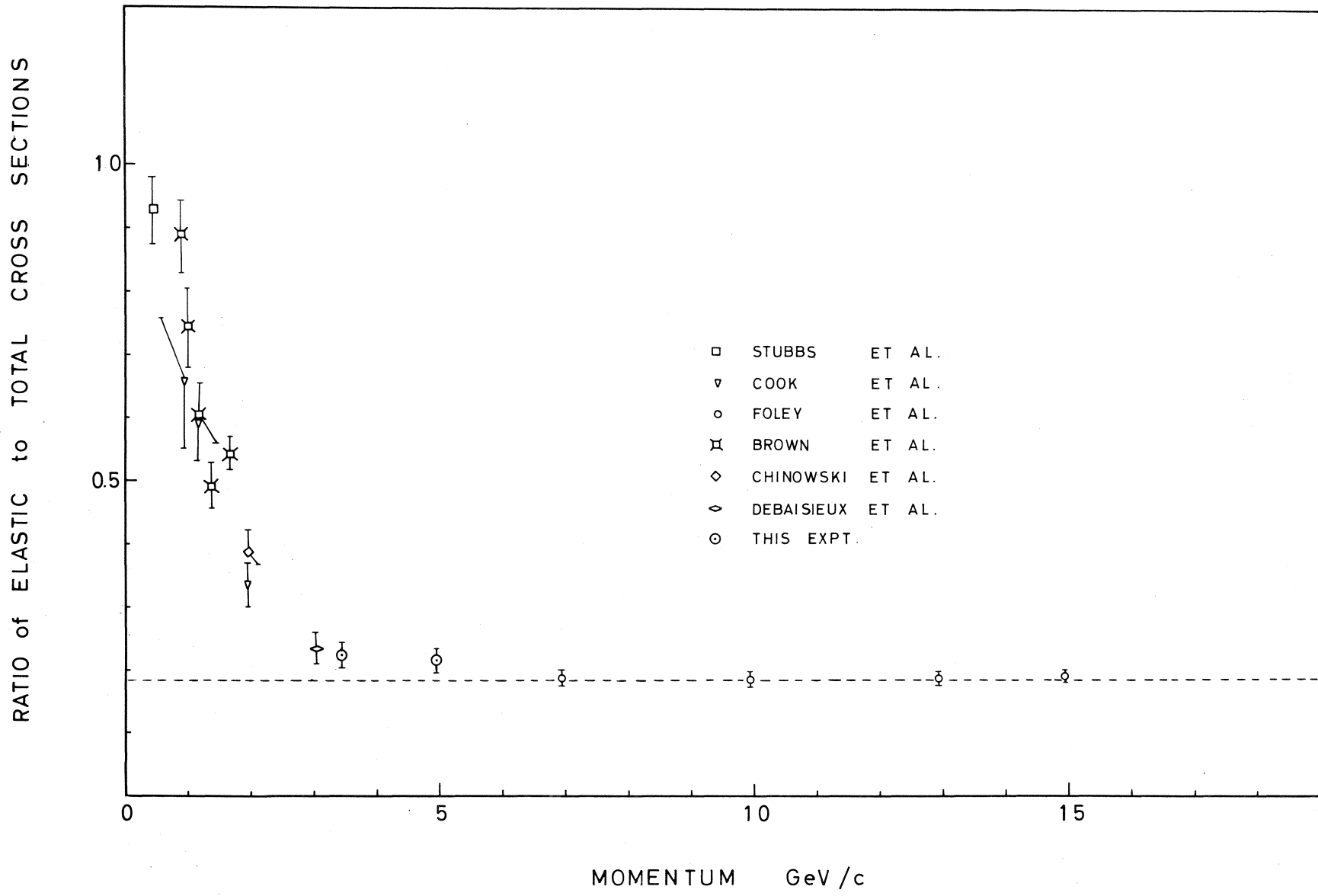


fig. 5



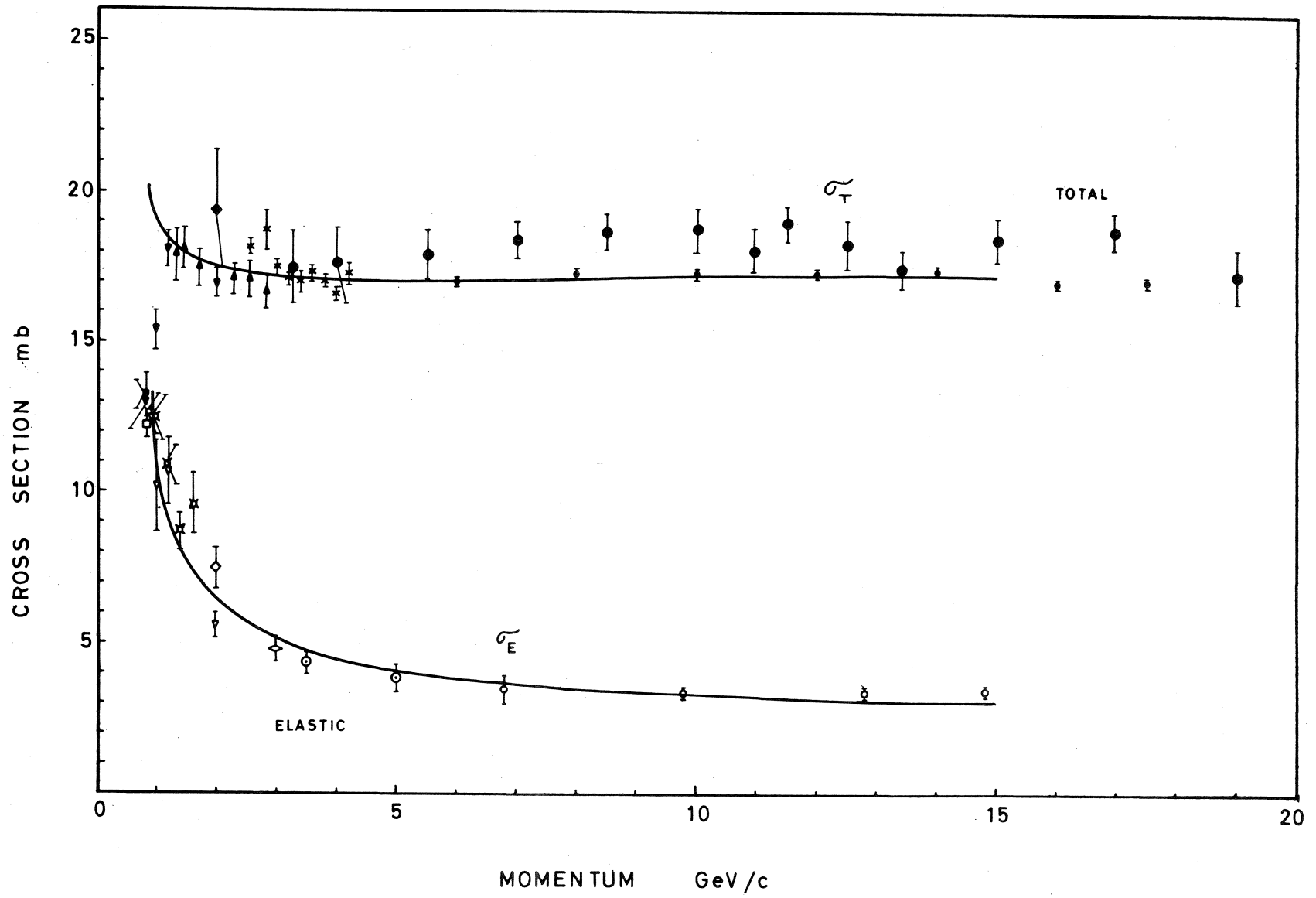


fig. 6

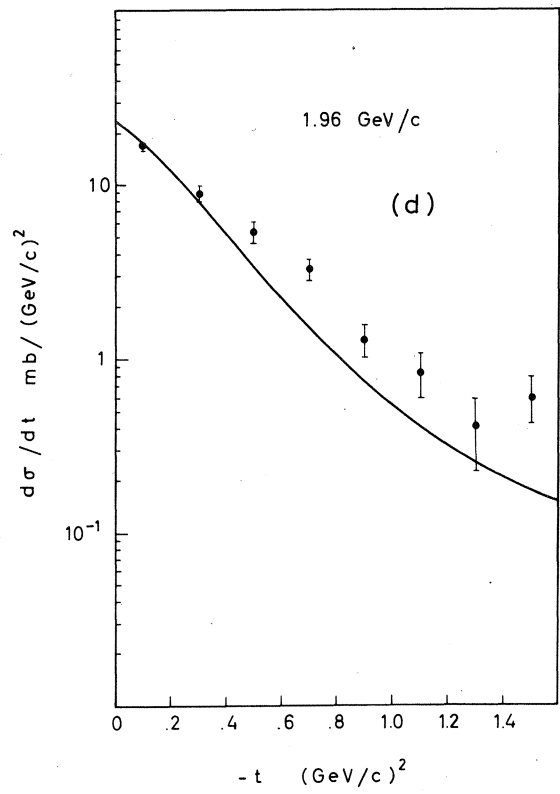
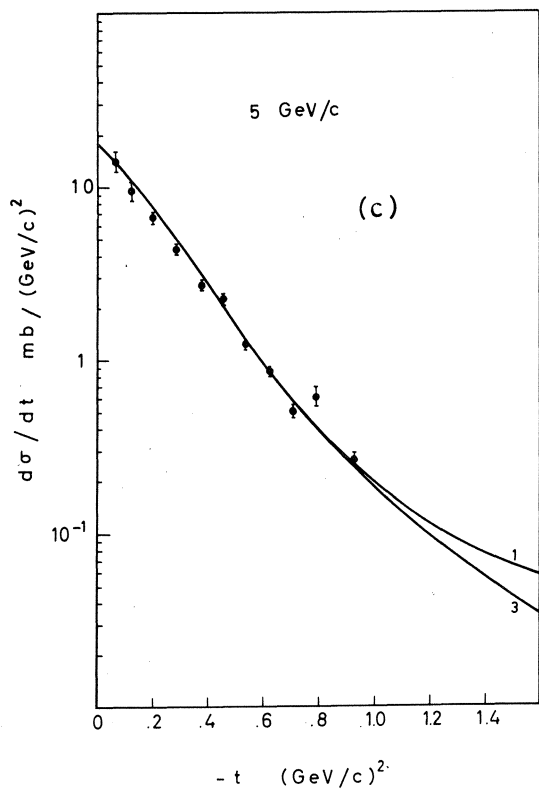
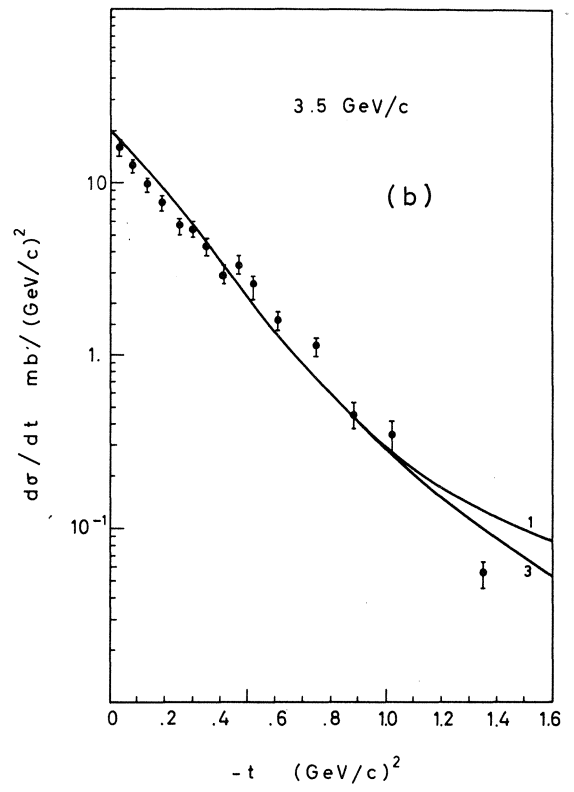
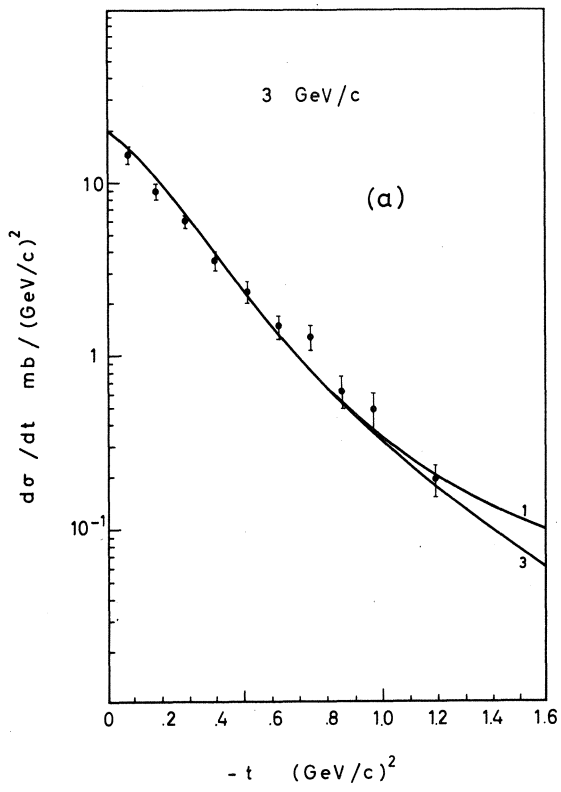


fig. 7